Genomics Communications

ARTICLE

Open Access

https://doi.org/10.48130/gcomm-0025-0002

Genomics Communications **2025**, 2: e002

An autotetraploid genome of *Corydalis sheareri* provides insight into the evolution and benzylisoquinoline alkaloids diversity of *Corydalis*

Yan-Yan Liu[1], Cheng-Long Yu[1], Yi-Jing Liu[1], Sheng-Long Kan[2], Min Chen[3], Ya-Nan Cao[1], Hong-Wei Wang[1*], Jia-Mei Li[4*] and Dan Peng[5,6*]

[1] *College of Plant Protection, Henan Agricultural University, Zhengzhou 450046, China*
[2] *Marine College, Shandong University, Weihai 264209, China*
[3] *Center for Plant Diversity and Systematics, Institute of Botany, Jiangsu Province and Chinese Academy of Sciences, Nanjing 210014, China*
[4] *College of Life Sciences, Henan Agricultural University, Zhengzhou 450046, China*
[5] *Shenzhen Branch, Guangdong Laboratory of Lingnan Modern Agriculture, Key Laboratory of Synthetic Biology, Laboratory of the Ministry of Agriculture and Rural Affairs, Agricultural Genomics Institute at Shenzhen, Chinese Academy of Agricultural Sciences, Shenzhen 518124, China*
[6] *School of Ecology, Hainan University, Haikou 570228, China*
* Corresponding authors, E-mail: whwcas@163.com; jiamei_li@126.com; 5220130045@fafu.edu.cn

Abstract

Corydalis DC. is the largest and most diverse genus of Papaveraceae, which has undergone rapid diversification. *Corydalis* is notable for its diverse benzylisoquinoline alkaloids (BIAs). However, limited genomic resources hinder the understanding of its evolution and BIA diversity. Here, we report a high-quality genome of *Corydalis sheareri* and provide a comparative analysis of *Corydalis* genomes. Genome survey shows that the genome of *C. sheareri* might be an autotetraploid. *De novo* assembly yields a single homolog genome of 282 Mb, with a contig N50 of 11.39 Mb. Repetitive DNA accounts for 44.47% of the genome, and a total of 26,287 protein-coding genes are predicted. When comparing this genome with the previously reported diploid genome of *C. tomentella*, large-scale structural variations are detected, which might have dramatic effects on the evolution of *Corydalis*. Furthermore, a total of 172 candidate genes involved in benzylisoquinoline alkaloids (BIAs) biosynthesis are identified in the genome of *C. sheareri*. Duplication and phylogenetic analyses indicate that tandem duplications play a prominent role in the evolution of the BIA biosynthesis genes, and might be associated with the BIA diversity in *Corydalis*.Our study provides more insights into the genome evolution and secondary metabolites diversity of *Corydalis*, and will accelerate genomic and evolutionary radiation study of species-rich plant genera.

Citation: Liu YY, Yu CL, Liu YJ, Kan SL, Chen M, et al. 2025. An autotetraploid genome of *Corydalis sheareri* provides insight into the evolution and benzylisoquinoline alkaloids diversity of *Corydalis*. *Genomics Communications* 2: e002 https://doi.org/10.48130/gcomm-0025-0002

Introduction

Corydalis DC. is the largest and most diverse genus of Papaveraceae, comprising more than 500 species, which are mainly divided into four subgenera (subg. *Bipapillatae*, subg. *Cremnocapnos*, subg. *Sophorocapnos*, and subg. *Corydalis*) and 39 sections[1]. *Corydalis* is widely distributed in the Northern Hemisphere with a few species extending into East Africa[2]. Moreover, this genus demonstrates remarkable diversity in China, particularly in the Himalaya–Hengduan Mountains and the adjacent regions[2,3]. As a genus with spectacular radiation, *Corydalis* exhibits an extremely high level of diversity in its leaves, subterranean organs, fruits, seeds, flower color, and the length of spurs, and can adapt to diverse habitats, such as riversides, forests, shrubs, grasslands, screes, or even cliffs. Previous studies speculated that *Corydalis* had an ancient origin, and underwent rapid radiation after the middle Miocene, which was most likely promoted by the continuous orogenesis and climate change associated with the uplift of the Qinghai-Tibetan Plateau (QTP)[4–7].

The sequencing of plant genomes has greatly advanced our understanding of the underlying diversification mechanisms[8–10]. Although considerable progress has been made recently in the classification and phylogeny of *Corydalis*, the underlying diversification mechanisms remain poorly understood. Particularly, polyploidy is common in this genus, suggesting that polyploidization possibly contributed to the diversification of *Corydalis*. Polyploidy could drive dramatic changes in the genome landscapes, such as genome size and structural variation, providing a genetic basis for the adaptation and diversification of species-rich groups. While more and more studies link polyploidization events with speciation, fewer studies have documented chromosomal variation in plant groups that underwent rapid radiations, thus the extent to which it may have contributed to radiation is still elusive, especially in biodiversity hotspots. In *Corydalis*, only the genomes of *C. tomentella* and *C. yanhusuo* have been released to date[11,12], which has hindered our understanding of its diversification and adaptation.

Moreover, a large number of *Corydalis* species have been frequently used in folk medicine due to their antibacterial, antiviral, and anticancer activities. For instance, *C. yanhusuo*, *C. bungeana,* and *C. decumbens* are the most famous medicinal plants recorded in the Pharmacopoeia of China (http://db.ouryao.com/yd2020/). High medicinal value of *C. sheareri*, *C. hendersonii*, *C. incisa*, *C. repens*, *C. edulis*, *C. racemosa,* and *C. pallida*, also have been reported[2]. Previous phytochemical investigations have isolated various components from *Corydalis*, including alkaloids, coumarins, flavonoids, anthraquinones, triterpenes, steroids, and organic acids[13]. Of particular interest are alkaloids, especially benzylisoquinoline alkaloids (BIAs), which have been reported to play a crucial role in sedation, releasing pain, promoting blood circulation, and inhibiting cancer cells[13]. Compared with other genera in Papaveraceae, *Corydalis* can produce multiple types of BIAs, such as cavidines, apocavidine, tetrahydropalmatine, corydalis, protopine, dehydroapocavidine, and dehydrocavidine. Notably, it was also reported that species-specific BIAs were also isolated in different species of

Corydalis[13–16], which indicates the remarkable diversity of BIAs in these plant groups. However, the limited genomic resources hampered an in-depth understanding of the diversity of BIAs in *Corydalis*. Fortunately, biosynthesis pathways of BIAs have been proposed in *Corydalis*[12,17], as well as in other Papaveraceae species, such as *Macleaya cordata*[18], *Eschscholzia californica*[19], and *Papaver somniferum*[20–22]. The biosynthesis of BIAs in *Corydalis* involves a series of enzymes, namely berberine bridge enzyme (BBE), berberine bridge enzyme-like (BBEL), C-methyltransferase (CMT), cytochrome P450 (CYP), norcoclaurine synthase (NCS), N-methylcoclaurine 30-hydroxylase (NMCH), coclaurine N-methyltransferase (CNMT), 4-hydroxyphenylpyruvate decarboxylase (HPPDC), O-methyltransferase (OMT), tyrosine aminotransferase (TAT), tetrahydroprotoberberine N-methyltransferase (TNMT), tyrosine decarboxylase (TYDC), and tyramine 3-hydroxylase (TYR).

In this study, PacBio long read sequencing, chromosome conformation capture (3C)-based Hi-C sequencing, and Illumina short-read sequencing were used to assemble a high-quality genome of *Corydalis shearei*, one species from subg. *Corydalis*, the largest and most diverse lineages of *Corydalis*. Genomic comparison was then carried out between *C. shearei* and *C. tomentella*, one previously reported diploid genome from subg. *Sophorocapnos*. Additionally, we identified the candidate BIAs biosynthesis genes in representative species in Papaveraceae and traced their evolution history by combing phylogenetic reconstruction, chromosomal location, and gene duplication analyses. Our study will provide more insights into the genome evolution as well as the BIAs diversity in *Corydalis*.

Materials and methods

Sample collection and genome sequencing

Fresh leaves, stems, rhizomes, and flowers at different developmental stages of *C. shearei* were collected from Zhongshan Botanical Garden (Nanjing, China) (Fig. 1a). After collection, these samples were immediately frozen in liquid nitrogen or dried in silica gel followed by preservation at −80 °C in the laboratory. The silica gel-dried leaves were used for the flow cytometry measurement, and the material stored in liquid nitrogen was used for genome and transcriptome sequencing. Genomic DNA was extracted using a modified CTAB method. Total RNA was extracted from leaves, stems, rhizomes, and flowers at different developmental stages using RNAprep Pure Plant Kit (Tiangen, Beijing).

For the genome survey, the 350 bp paired-end library was constructed according to the Illumina protocols and sequenced on the Illumina Novaseq 6000 platform. For PacBio HiFi sequencing, the DNA SMRT bell library with an insert size of approximately 15 kb was prepared using SMRTbell® Express Template Prep Kit 2.0 (Pacific Biosciences, PN 101-853-100), and subsequently sequenced on the PacBio Sequel II platform (Pacific Biosciences, USA). For high-throughput 3C-based Hi-C sequencing, the library was generated using the standard procedures and sequenced on the Illumina Novaseq 6000 platform. For transcriptome sequencing, RNA from different tissues was pooled equally for library construction to obtain more expressed genes. Thereafter, the cDNA library with an insert size of 300–500 bp was prepared using VAHTS mRNA-seq v2 Library Prep Kit for Illumina (Vazyme) and sequenced on the Illumina Novaseq 6000 platform to generate paired-ends reads. All sequencing was carried out in Berry Genomics Company (www.berrygenomics.com), Beijing, China. The raw Illumina data for genome survey, Hi-C, and RNA-seq reads, was trimmed using Fastp v0.23.2[23] to remove the adaptors and low-quality paired reads. The HiFi reads were generated through CCS software (https://github.com/PacificBiosciences/ccs) with the following parameters: --min-passes = 3 --min-rq = 0.99.

Genome survey

To guide genome sequencing and assembly, flow cytometry[24], and genome survey were used to estimate the genome size. For flow cytometry, the dried material was chopped with a razor blade and then the DNA content was measured following the protocol of CyStain®PI Absolute P (Sysmex-Partec, Germany) with an Elite flow cytometer (BD FACSCalibur, USA) at the Institute of Botany, Chinese Academy of Sciences (China). Finally, the genome size was inferred based on the external reference standards (*Glycine max* = 1,100 Mb). For genome survey, the obtained clean reads were used to estimate the genome size based on the *k-mer* method with KMC v3[25], and Genomescope v2.0[26]. Given that multiple peaks were detected in the *k-mer* spectrum, Smudgeplot[26] was further employed to visualize and evaluate the ploidy and genome structure through the analysis of heterozygous *k-mer* pairs.

Genome assembly and annotation

Hifiasm v0.14.2[27] was used for *de novo* assembly of the draft contig genome of *C. shearei*, which contained unphased contigs from two homolog genomes (csh v1.0). Purge_dups v1.2.3[28] was used to improve the assembly by removing duplications. The filtered Hi-C reads were aligned to the draft genome (csh v1.0) using Juicer v1.6.2[29], and scaffolding was performed on the contigs with 3D-DNA v180922[30]. Juicebox v1.9.8[31] was used to visualize the Hi-C heatmap, and the scaffolds were manually adjusted to get the chromosomal-level assembly of *C. shearei* (csh v2.0). BWA v0.7.15[32] and minimap2[33] were used to assess the quality of the genome by aligning the Illumina short reads and the long HiFi reads to the genome, respectively. BUSCO v4.14[34] was performed to evaluate the integrity of the assembled genome by searching against the 1,614 conserved single-copy genes obtained from the embryophyta_odb10 database.

LTR_Finder v1.07[35], MITE-Hunter v1.0[36], and Repeat-Masker v4.1.0 (www.repeatmasker.org) were used to predict the repeat sequences. Protein-coding genes were predicted by combining the results of *ab initio*-based, homology-based, and RNAseq-based predictions. For *ab initio* prediction, Augustus v3.2.2[37], Snap v6.0[38], Glimmer hmm v3.0.4[39], and GeneMark-ET v4.57[40] were utilized to predict the gene structure in the repeat-masked genome. GeMoMa v1.7.1[41] was used to perform homology prediction with *Arabidopsis thaliana*, *Oryza sativa*, *Macleaya cordata,* and *Papaver rhoeas* as references. For RNAseq-based prediction, transcriptomic data from different tissues were assembled *de novo* using trinity v2.2.0[42]. PASA r20140417[43] was used to predict the gene structure based on the obtained transcript. All predicted protein-coding genes were annotated by blast against five databases, including KEGG (www.genome.jp/kegg/brite.html), Gene Ontology (GO) terms, NR (https://ftp.ncbi.nlm.nih.gov/blast/db/FASTA/nr.gz), SwissProt (https://ftp.uniprot.org/pub/databases/uniprot/current_release/knowledgebase/complete/uniprot_sprot.fasta.gz), and eggNOG (http://eggnog5.embl.de/#/app/home). The tRNA (transfer RNA) was predicted by tRNAscan-SE v2.0[44]. Other types of noncoding RNAs (ncRNAs), including rRNA (ribosomal RNA), miRNA (microRNA), and snRNA (small nuclear RNA), were annotated by BLAST against the Rfam database (https://ftp.ebi.ac.uk/pub/databases/Rfam/14.1/).

Phylogenomic analysis and whole-genome duplication (WGD) identification

Eight species from Papaveraceae were selected for phylogenomic analysis, including *C. shearei*, *C. tomentella*, *Eschscholzia californica*,

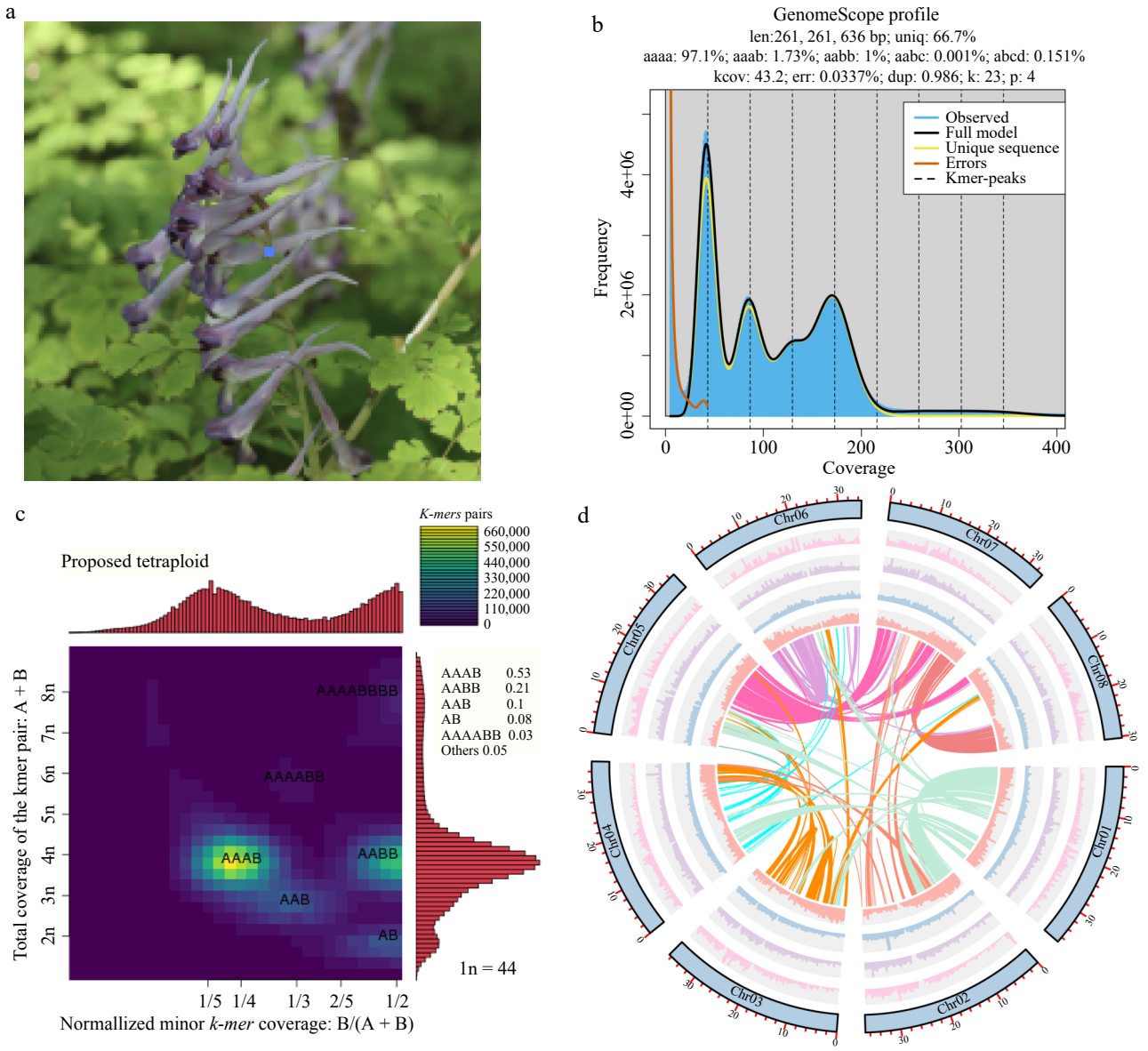

Fig. 1 Overview of *Corydalis shearer*i genome. (a) Photo of *C. shearer*i. (b) Genome survey of *C. shearer*i. (c) Heatmap for coverage pattern of heterozygous *k-mer* pairs, in which X axis indicates the normalized minor *k-mer* coverage, while Y axis indicates the total *k-mer* pairs coverage. (d) Genomic features of eight pseudochromosome. The outermost circle (blue) represents each chromosome of the genome. The bar charts of the second to fifth circles suggest gene density, LTR density, *Copia,* and *Gypsy* density, respectively. The inner circular shows inter-chromosomal synteny.

Macleaya cordata, *Papaver somniferum*, *Capnoides sempervirens*, *Ceratocapnos vesicaria*, and *Hypecoum procumbens*, with *Aquilegia coerulea* (Ranunculaceae) as outgroup. The genomes or transcriptomes were directly retrieved from Genome Warehouse in National Genomics Data Center (https://ngdc.cncb.ac.cn/gwh), National Center for Biotechnology Information (www.ncbi.nlm.nih.gov/datasets/genome), and ONEKP database (https://db.cngb.org/onekp). Gene families were clustered using protein sequences by OrthoFinder v2.2.7[45] with the parameter '-S diamond' . Each gene family was aligned with MAFFT[46]. Single or low-copy gene families (one or two copies in the polyploid species *Papaver somniferum*, while one copy in the other eight species) with more than 50 amino acids were retained to reconstruct the phylogenetic tree by RAxML v8.1.17[47] with 1,000 bootstrap replicates under PROTCATWAG model using protein sequences. Divergence time was estimated under a relaxed molecular clock model by the MCMCTree implement in the PAML v4.8[48]. Calibration points retrieved from TimeTree (http://timetree.org) were used as priors in divergence time estimation, including the split of Papaveraceae and Ranunculaceae (103~117 Ma), the crown age of Papaveraceae (65~111 Ma), the split age of Hypecoideae and Fumarioideae (63~96 Ma) and the crown age of Fumarioideae (38~44 Ma). Gene family expansion and contraction were inferred by CAFE v4.1[49], with an input species tree constructed from the single or low-copy orthologs. Meanwhile, we performed functional enrichment analysis for the expanded gene families by BLAST against the KEGG and GO databases.

The whole-genome duplication (WGD) and whole-genome triplication (WGT) events were identified by *Ks* method, syntenic analyses, and phylogenomic methods. For *Ks* method, the homologous gene pairs were firstly identified by the all-against-all BLASTP search (e-value cutoff < 1e-5). Then, YN00 in PAML v4.8[48] was called by WGDI[50] to calculate the synonymous substitution rate (*Ks*) of each gene pair between two species or within a single species. For

syntenic analyses, collinear blocks for intra- and interspecies comparisons were detected using MCScanX v0.8[51] with '-s 15', meaning that each block contained at least 15 collinear gene pairs. JCVI v0.8.12[52] was used to draw dotplots of *C. sheareri*, *C. tomentella*, *V. vinifera,* and *A. trichopoda* with the default parameters. TBtools[53] was used to visualize the synteny between *C. sheareri* and *C. tomentella*. Additionally, structural variants between *C. sheareri* and *C. tomentella*, i.e., inversion, translocation, and duplication, were identified with SyRI v1.6.3[54]. For phylogenomic methods, gene families were firstly identified by OrthoFinder v2.2.7[45] and multiple sequence alignments were performed by MAFFT[46]. Then, Maximum-Likelihood (ML) trees were constructed using RAxML[47], with bootstrap values estimated from 100 replicates using the PROTCAT-WAG model. The WGD/WGT event was identified by tree2GD (https://sourceforge.net/projects/tree2gd/) with the default parameter and WGD/WGT events were considered to have occurred according to any of the following conditions: (1) gene duplication (GD) > 500, of which the number of (AB)(AB) type is over 250; (2) GD > 1,500, of which (AB)(AB) type is over 100, and at the same time, the sum of (AB)(AB) type and (AB)A or (AB)B type are over 1,000[55].

Evolution of BIA biosynthesis-related gene family

To gain more insights into the diversity of BIAs in *Corydalis*, 12 gene families involved in BIAs biosynthesis, i.e., *BBE*, *BBEL*, *CMT*, *CYP719*, *CYP80B*, *CYP82N*, *NCS*, *NMT*, *OMT*, *TAT*, *TYDC,* and *TYR*, were identified. All BIA biosynthesis genes reported in *C. tomentella* genome were firstly retrieved by the gene ID reported previously[12]. Then, TBLASTN was conducted to identify the candidate BIA-related genes in *C. sheareri* and seven other species of Papaveraceae, including *Chelidonium majus*, *Capnoides sempervirens*, *Ceratocapnos vesicaria*, *Hypecoum procumbens*, *Eschscholzia californica*, *Macleaya cordata*, *Papaver somniferum*, with *Aquilegia coerulea* as the outgroup. A sequence is regarded as a candidate gene if it encompasses the entire domain region and the pairwise amino acid identity between the queries and the targets exceed 40%. The annotation for each candidate gene was manually checked according to the blast result. All candidate sequences were confirmed by BLAST against the InterPro (www.ebi.ac.uk/interpro/) and the NCBI Conserved Domain Database (CDD, www.ncbi.nlm.nih.gov/Structure/cdd/wrpsb.cgi) with e < 1e-10.

To infer the expansion mechanism of the BIAs biosynthesis genes, phylogenetic reconstruction, chromosomal location, and gene duplication analyses were performed. ML analyses were conducted based on the protein sequences by IQ-TREE v1.6.8[56] using the JTT model and 100 bootstrap replications. Gff files, gene files, and targeted BIA biosynthesis gene IDs of *C. sheareri* and *C. tomentella* were downloaded or extracted. The chromosome location information was obtained from the genome annotation file, and visualized by TBtools[53]. Gene duplication events were analyzed using MCScanX[51] with a BLASTp search (e < 1e-10). The synonymous (*Ks*) and nonsynonymous (*Ka*) values of the identified species-specific tandem duplicated gene pairs were calculated by the M0 model in PAML v4.8[48].

Results

Genome assembly and annotation

Flow cytometry indicated that *C. sheareri* had a genome size of approximately 580 Mb (Supplementary Fig. S1a). Based on the obtained 66.29 Gb short paired-end reads (Supplementary Table S1), the 23-mer distribution showed that the estimated genome size of *C. sheareri* was 261 Mb (Fig. 1b), and the *k-mer* spectrum exhibited four distinct peaks at ~40, 80, 120, 160, which was highly similar to the results for autotetraploids (*M. sativa* and *S. spontaneum*)[26]. Moreover, nucleotide heterozygosity analysis showed 1.73% *aaab* and 1% *aabb*, which was consistent with the expectation that the heterozygous rate of autotetraploid AAAB would be greater than that of AABB[26]. The Smudgeplot analysis also revealed that more heterozygous *k-mer* pairs concentrated at 1/4 for the normalized coverage of minor *k-mer* and 4n for the total coverage of *k-mer* pairs, and the prevalence of AAAB (53%) was considerably greater than AABB (21%) (Fig. 1c). All these results suggested that the genome of *C. sheareri* exhibited complex genome structure and possibly an autotetraploid.

PacBio Sequel II sequencing yielded approximately 33.02 Gb of high quality Hifi reads, and the average length and N50 of filtered subreads (1,990,989) were 16,584 bp and 16,614 bp, respectively (Supplementary Table S1). *De novo* assembly generated the draft genome of *C. sheareri* (csh v1.0, ~550 Mb) with contig N50 of 9.18 Mb, and the longest contig was approximately 25.09 Mb (Table 1). The assembly was further scaffolded with 67.96 Gb Hi-C data (Supplementary Table S1). Finally, the high-quality genome of *C. sheareri* (csh v2.0, ~282 Mb) comprised eight pseudochromosomes and 36 contigs (Supplementary Fig. S1b, Supplementary Table S2), with contig N50 of 11.39 Mb (Table 1). The minimum length of the chromosome was greater than 30 Mb (Supplementary Table S2). Approximately 97.62% of DNA reads and 88.32% of RNA-seq reads could be mapped to the assembly genome. BUSCO analysis revealed that 97.1% (1,567/1,614) of the core eukaryotic genes were completely present in the *C. sheareri* genome, of which 91.4% were single copy (1,475) and 5.7% were duplicated (92), while 0.9% (15), and 2.0% (32) were partially present or missing, respectively.

Approximately 44.47% (125,404,725 bp) of the *C. sheareri* genome was annotated as transposable elements (TEs), of which 26.47% were retrotransposons and 7.37% were transposons (Supplementary Table S3). For retrotransposons, a total of 84,322 LTR elements were identified, of which 53,097 (7.27%) belonged to the *Copia* superfamily and 29,747 (5.05%) belonged to the *Gypsy* superfamily (Supplementary Table S3). Based on a combination of homology search, *de novo* prediction, and RNA-seq based prediction, a total of 26,287 protein-coding genes were confidently annotated for *C. sheareri*, and the mean lengths of the predicted gene and coding sequence were 5,092 and 1,440 bp, respectively (Table 1). Approximately, 92.39% (24,286/26,287) of the genes were functionally annotated, of which, 24,257, 19,162, 8,566, 5,531, and 23,330 genes showed high similarity to known proteins in the NR, SwissProt, KEGG, GO, and eggNOG databases, respectively (Supplementary Fig.

Table 1. Genome assembly and annotation of *Corydalis sheareri.*

Analytical process	Characteristic	*C. sheareri*
Genome survey	Genome size (flow cytometry) (Mb)	580
	Genome size (*k-mer* spectrum) (Mb)	261
Assembly_csh v1.0	Number of contigs	2,713
	Assembly size (Mb)	550
	Contig N50 (Mb)	9.18
	Shortest contig (bp)	16,037
	Largest contig (bp)	25,090,490
Assembly_csh v2.0	Total number of contigs	179
	Assembly size (Mb)	282
	Contig N50 (Mb)	11.39
	Number of pseudochromosomes	8
	GC content	37.11%
Annotation	Number of protein-coding genes	26,287
	Mean gene length (bp)	5,092
	Mean CDS length (bp)	1,440
	Complete BUSCOs (C)	1,567
	Percentage of repeat sequences (%)	44.47

S2). In addition, a total of 2,746 noncoding RNA genes were identified in the genome of *C. shearei*, including 1,014 tRNA genes, 919 rRNA genes, 609 snRNA genes, and 86 miRNA genes (Supplementary Table S4).

Genome evolution

A total of 28,545 orthologous groups (OGs) were identified in nine selected species (Fig. 2b, Supplementary Table S5). Of them, 7,769 gene families were shared by all species, while 1,714 gene families were specific to *Corydalis*. Additionally, 1,025 single or low-copy nuclear gene families were identified in these species. After removing the OGs less than 50 aa, 1,003 single or low-copy nuclear gene families were retained to infer a high-confidence species tree. As expected, three subfamilies were recovered in the phylogenomic analysis, and Hypecoideae was strongly supported as a sister to Fumarioideae. Within Fumarioideae, *C. shearei* and *C. tomentella* formed a highly supported clade, while the relationship of *Ceratocapnos vesicaria*, *Capnoides sempervirens,* and *Corydalis* was not fully resolved. Within Papaveroideae, *Eschscholzia californica* diverged firstly, and *Papaver somniferum* was sister to *Macleaya cordata* (Fig. 2a). Molecular dating indicated that the divergence of *C. shearei* and *C. tomentella* was dated to 24.92 Ma, with a 95% confidence interval (95% CI) of 16.35~33.22 Ma (Fig. 2a). Gene family expansion and contraction analyses revealed that 674 and 566 gene families expanded and contracted in *Corydalis*, respectively (Fig. 2a). GO and KEGG enrichment analyses showed that the significantly expanded gene families were mainly related to response to stimulus, membrane, cell periphery, response to chemical, and cellular response to stimulus, which primarily enriched in secondary metabolites pathways such as phenylpropanoid biosynthesis, pentose, and glucuronate interconversions, photosynthesis, flavonoid biosynthesis, and monoterpenoid biosynthesis (Supplementary Fig. S3). Specifically, cytochrome P450 (CYP) and photosynthesis proteins were also enriched in the KEGG analysis (Supplementary Fig. S3).

WGD events play a crucial role in the duplication and retention of genes. Intra-genomic colinearity analyses uncovered remnants of one WGD event in *C. shearei* (Fig. 2c). Obviously, one signature peak of synonymous substitutions per synonymous site (*Ks*) distribution was detected for the *C. shearei* genome at approximately 1.0 (Fig. 2d), indicating an ancient WGD event. Similarly, previously sequenced genomes of Ranunculales species, including *C. tomentella,* and *A. coerulea*, also showed a signature peak at 1.0~1.2 in their genomes (Fig. 2d), suggesting this WGD event was probably shared by all Ranunculales species. Comparison of the *C. shearei* paralogue *Ks* distribution between *Corydalis* and *Aquilegia coerulea* also indicated a WGD occurred in Ranunculales (Fig. 2d). Previous studies reported that the *Vitis vinifera* genome had an ancestral hexaploidization[57] and the *Amborella trichopoda* genome shows no

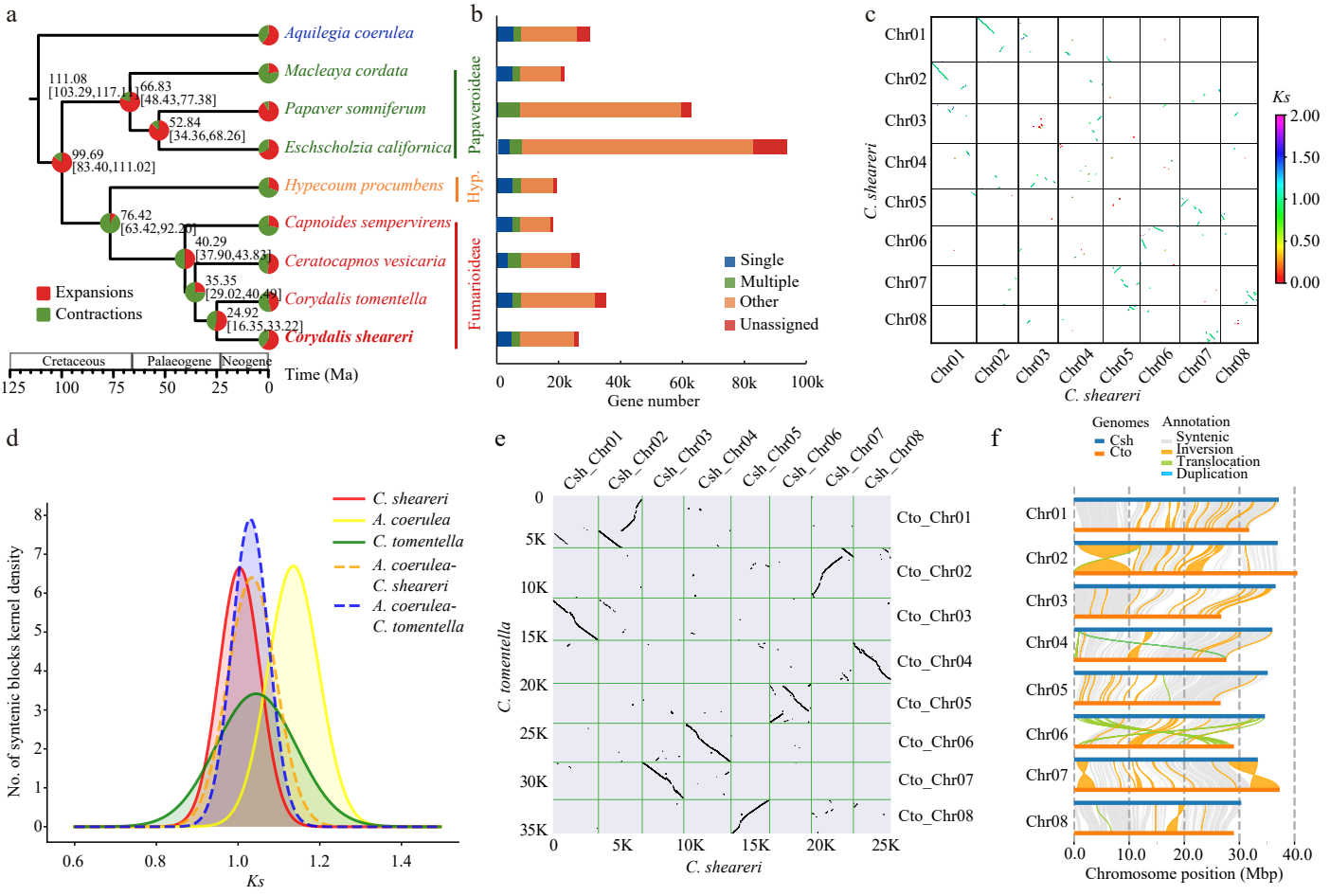

Fig. 2 Genome evolution of *Corydalis shearei*. (a) Phylogenetic tree and divergence time estimation. Pal., Palaeogene; Neo., Neogene; Hyp., Hypecooideae. (b) Gene families identified in each species. (c) Collinearity within the genome of *C. shearei*. (d) *Ks* distributions of anchor pairs for the paralogous genes of *C. shearei*, *C. tomentella* and *Aquilegia coerulea*, and for orthologous genes between *C. shearei* and *C. tomentella*, *A. coerulea*, respectively. (e) Collinearity analysis between *C. shearei* and *C. tomentella*. (f) Structural variation detection between *C. shearei* and *C. tomentella* performed by SyRI.

evidence of more recent lineage-specific genome duplications[58]. The inter-genomic comparison and syntenic depths analyses among *Corydalis shearei, Vitis vinifera,* and *Amborella trichopoda* further confirmed that this ancient WGD event, in which two paralogous segments in the *Corydalis shearei* genome correspond to one and three orthologous regions in the *Amborella trichopoda* (with no WGD), and *Vitis vinifera* (with one WGT) genomes, respectively (Supplementary Fig. S4). The tree2GD analyses revealed 1,281 GDs with 934 (73%) (AB)(AB) retention type, which also strongly suggested the identified WGD event was shared by the ancestor of Ranunculales (node 5) (Supplementary Fig. S5). The genome of *Corydalis shearei* and *C. tomentella* exhibited good collinearity (Fig. 2e, f, Supplementary Fig. S6). A number of large structural variations were detected, including multiple invasions across the genome, and a small fraction of translocations on chromosomes 6 (Fig. 2f). To further verify the authenticity of these structural variations, several specific inversion regions were randomly checked by mapping the HiFi reads to the assembled genome with Integrative Genomics Viewer (IGV)[59]. Our results confirmed that these inversions are genuine and not assembly artifacts (Supplementary Fig. S7).

Chromosomal location and gene duplication of BIAs biosynthesis genes in *Corydalis*

A total of 172 genes involved in the BIAs biosynthesis have been identified in *Corydalis shearei*, which is notably larger than that found in *C. tomentella* (125), *Macleaya cordata* (128), and *Aquilegia coerulea* (138), while smaller than that observed in *Papaver somniferum* (364) and *Eschscholzia californica* (197) (Fig. 3b; Supplementary Table S6), which has undergone two WGD events[12]. For each gene family, the upstream BIA biosynthetic genes, such as *TAT*, *TYDC*, *TYR*, *BBE,* and *CYP80B* (*NMCH*), generally possess small copy numbers in *Corydalis*. Conversely, the downstream BIA biosynthetic genes, including *OMT*, *CMT*, *NMT*, and *BBEL*, typically have a higher copy number (Fig. 3b; Supplementary Table S6). The only exception is NCS, which encodes enzymes to catalyze the condensation of dopamine and 4-hydroxyphenylacetaldehyde (4-HPAA) to produce norcoclaurine, in the upstream of BIA biosynthesis, which also has a greater number of copies (Fig. 3a, b).

Chromosomal location analysis indicated that some BIA biosynthetic genes are unevenly distributed among chromosomes. For instance, all 22 *NCS* genes of *C. shearei* are located on chromosome 6, whereas, in *C. tomentella*, all members are mapped on the chromosome 5. Additionally, in *C. shearei*, 34 out of the 39 *BBEL* genes are located on chromosome 4, 17 out of the 22 *NMT* genes are mapped on the chromosome 6, and nine out of 15 *CYP82N* genes are found on chromosome 3 (Fig. 4a). Similarly, in *C. tomentella*, 25 out of 31 *BBEL* genes are found on chromosome 6, and 15 out of the 20 *NMT* genes are located on chromosome 5 (Fig. 4b). On the contrary, some other genes are widely distributed throughout genomes but are uneven among chromosomes in both two species. For instance, seven out of eight chromosomes (except for chr02)

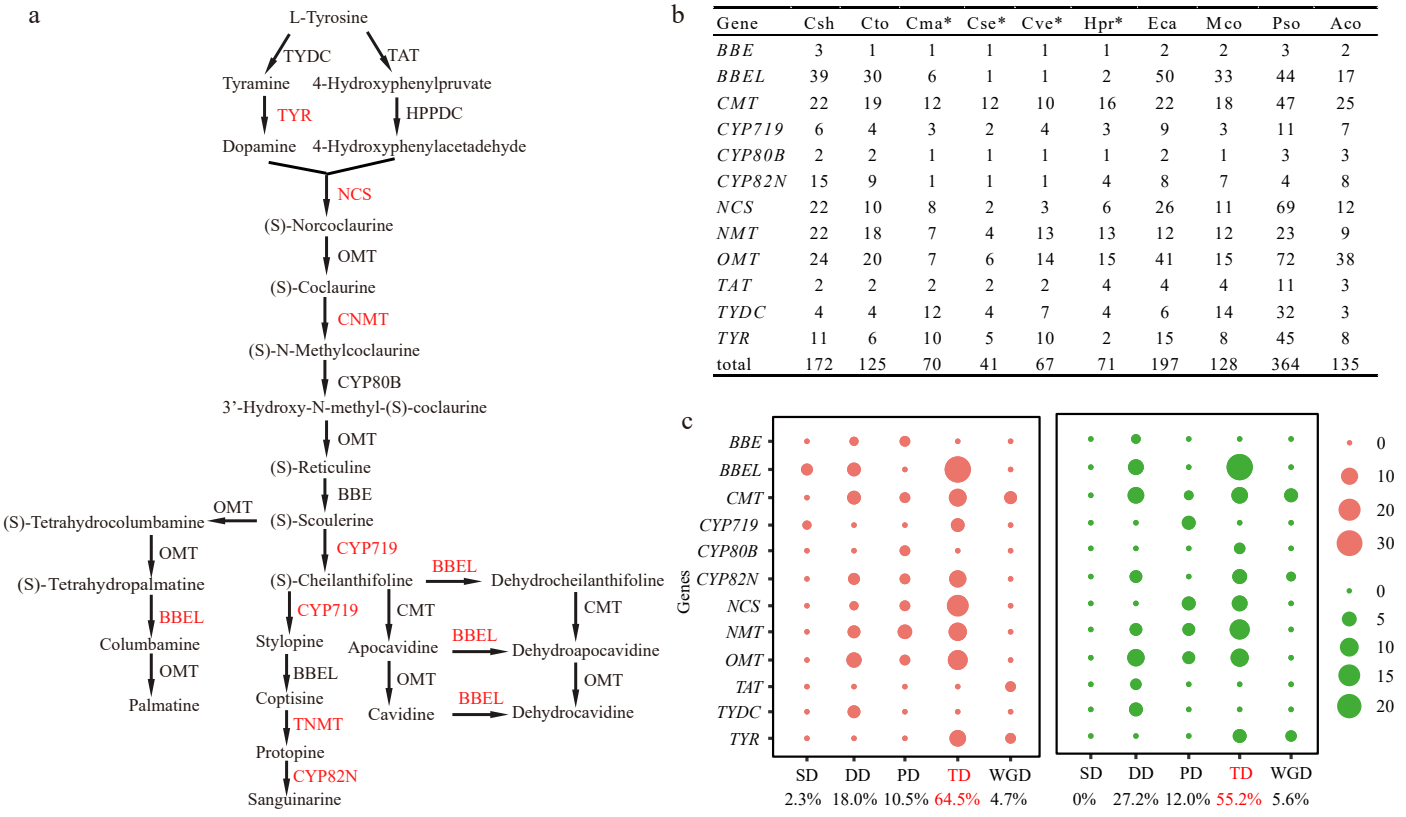

Gene	Csh	Cto	Cma*	Cse*	Cve*	Hpr*	Eca	Mco	Pso	Aco
BBE	3	1	1	1	1	1	2	2	3	2
BBEL	39	30	6	1	1	2	50	33	44	17
CMT	22	19	12	12	10	16	22	18	47	25
CYP719	6	4	3	2	4	3	9	3	11	7
CYP80B	2	2	1	1	1	1	2	1	3	3
CYP82N	15	9	1	1	1	4	8	7	4	8
NCS	22	10	8	2	3	6	26	11	69	12
NMT	22	18	7	4	13	13	12	12	23	9
OMT	24	20	7	6	14	15	41	15	72	38
TAT	2	2	2	2	2	4	4	4	11	3
TYDC	4	4	12	4	7	4	6	14	32	3
TYR	11	6	10	5	10	2	15	8	45	8
total	172	125	70	41	67	71	197	128	364	135

Fig. 3 BIAs biosynthesis related gene families identified in this study. (a) The biosynthetic pathway of benzylisoquinoline alkaloids (BIAs) in *Corydalis*. The species-specific tandem duplicated gene pairs or clusters in *Corydalis* identified in Fig. 5 and Table 2 were highlighted with red color. (b) The copy number of BIAs biosynthesis related gene families. Four species with transcriptome sequence are represented by asterisks. (c) Gene duplication type identified in *C. shearei* (left) and *C. tomentella* (right). Abbreviations: BBE, berberine bridge enzyme; BBEL, berberine bridge enzyme-like; CMT, C-methyltransferase; CNMT, coclaurine N-methyltransferase; CYP, Cytochrome P450; HPPDC, 4-hydroxyphenylpyruvate decarboxylase; NCS, norcoclaurine synthase; NMT, N-methyltransferase; OMT, O-methyltransferase; TAT, tyrosine aminotransferase; TNMT, tetrahydroprotoberberine N-methyltransferase; TYDC, tyrosine decarboxylase; TYR, tyramine 3-hydroxylase. Aco, *Aquilegia coerulea*; Cma, *Chelidonium majus*; Cse, *Capnoides sempervirens*; Csh, *Corydalis shearei*; Cto, *C. tomentella*; Cve, *Ceratocapnos vesicaria*; Eca, *Eschscholzia californica*; Hpr, *Hypecoum procumbens*; Mco, *Macleaya cordata*; Pso, *Papaver somniferum*. SD, Singleton; DD, dispersed duplications; PD, proximal duplications; TD, Tandem duplications; WGD, segmental/WGD duplications.

harbor the 22 *CMT* genes in *C. sheareri*, and 11 of them are located on chromosome 4. Furthermore, five chromosomes (1, 2, 4, 6, and 8) contain the *OMT* genes, and both chromosome 2 and 4 harbor nine members (Fig. 4a). In *C. tomentella*, 20 *OMT* genes are distributed across five chromosomes (1, 2, 4, 5, and 6). and chromosome 6 harbors eight members, chromosome 1 harbors four (Fig. 4b). Nineteen *CMT* genes are located on seven chromosomes (except for chr01), and 9 of them are located on chromosome 8 (Fig. 4b). Interestingly, a gene cluster including seven *NCS* genes and ten *NMT* genes, was identified in chromosome 6 within a 270-kb region of *C. sheareri* genome (Fig. 4a).

Gene duplication analysis revealed that the majority of BIAs biosynthesis genes were generated through gene duplication events in *Corydalis*. Over half of these genes were identified as tandem duplications, with 55.2% in *C. tomentella* and 64.5% in *C. sheareri*, respectively (Fig. 3c; Supplementary Table S6). Additionally, 18% to 27.2% of genes were identified as dispersed duplications, and one-tenth of genes, corresponding to 10.5% to 12.0%, were

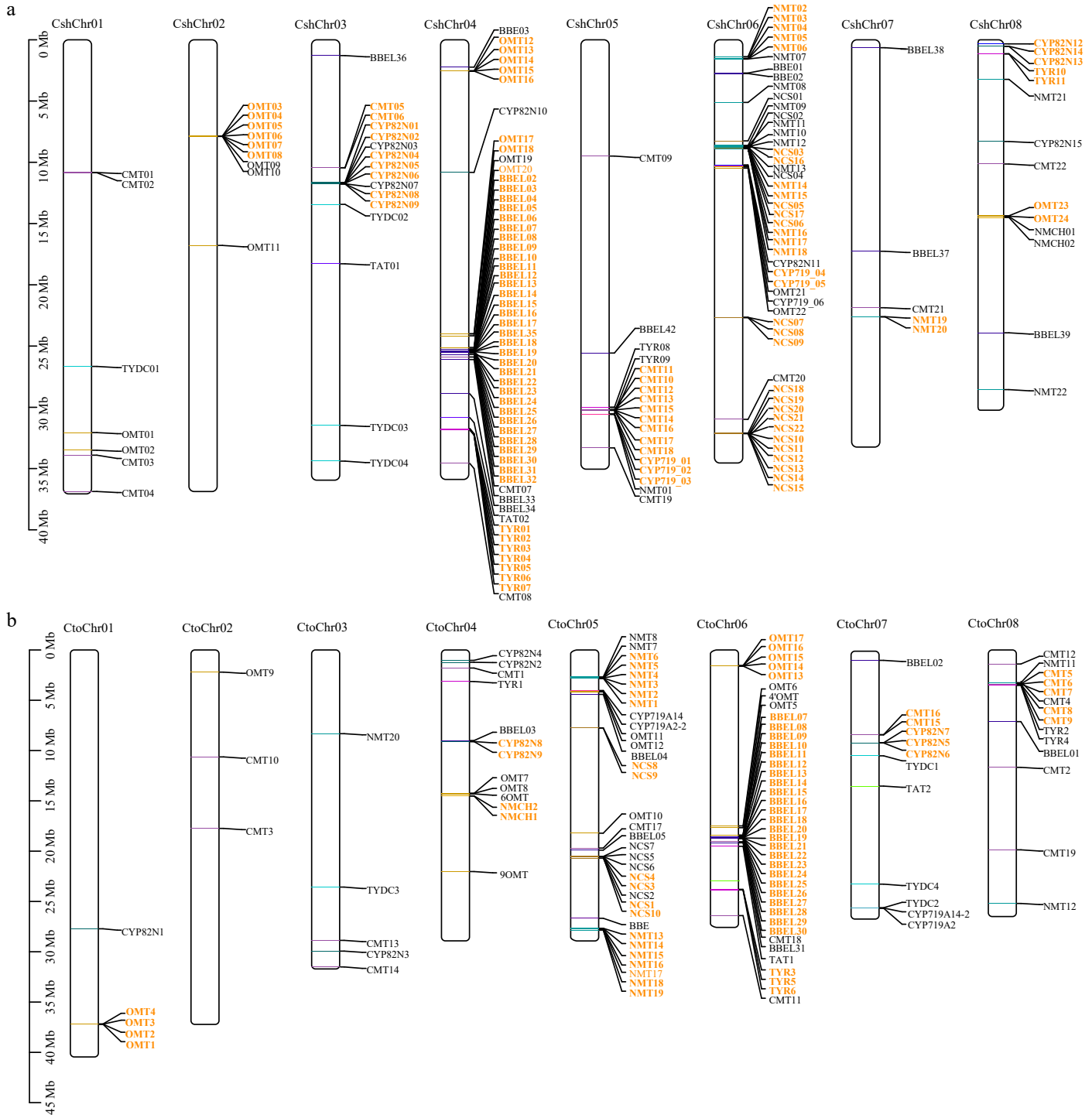

Fig. 4 Chromosome location and duplication event analyses of BIA biosynthesis genes in (a) *C. sheareri* and (b) *C. tomentella*. The chromosome number is indicated at the top of each chromosome. Tandem duplicated genes are indicated with orange color. The scale bar on the left indicates the length (mb) of chromosomes. The gene and species abbreviations were the same as Fig. 3. Chr, chromosome.

recognized as proximal duplications (Fig. 3c; Supplementary Table S6). Meanwhile, a small fraction, ranging from 4.7% to 5.6%, were identified as segmental/WGD (Fig. 3c; Supplementary Table S6). Specifically, *BBEL* genes exhibit an extremely high probability of tandem duplication in both *C. sheareri* and *C. tomentella*. For instance, 31 *BBEL* genes (79.4%) of *C. sheareri* were found to be tandemly duplicated on chromosome 4, while 24 members (80%) of *C. tomentella* tandemly duplicated on chromosome 6 (Figs 3c, 4; Supplementary Table S6). Moreover, *NCS*, *CYP719*, and *TYR* genes also demonstrated an extremely high rate of tandem duplication in *C. sheareri*, with 19 out of 22 *NCS* genes (86%), five out of six *CYP719* genes (83%) and nine out of 11 *TYR* genes (82%) were observed to be tandemly duplicated (Figs 3c, 4a; Supplementary Table S6).

Phylogeny of genes involved in BIAs biosynthesis

Among the genes associated with the BIAs biosynthesis, the largest is the *BBEL* family, with 39 members in *Corydalis sheareri* and 30 members in *C. tomentella*, respectively (Fig. 3b; Supplementary Table S6). Phylogenetic analysis of *BBE* and *BBEL* revealed three monophyletic clades (BBE, I, and II). Clade II has undergone a significant expansion in *Corydalis*, encompassing 34 members from *C. sheareri* and 23 from *C. tomentella*. Seven *C. sheareri* or *C. tomentella*-specific monophyletic groups were identified in clade II, and one of them comprised a notably high number of 14 members from *C. sheareri* (Fig. 5a).

CYPs are important for determining chemical diversity in metabolism, in which, *CYP719*, *CYP80B* (*NMCH*), and *CYP82N*, have been identified as key components of BIA biosynthesis[12,60,61]. Phylogenetic analysis of these three CYP subfamily suggested that 13 *CYP82N* genes of *C. sheareri* (a total of 15 members) were clustered into four monophyletic groups, and two members of *C. tomentella* (*CtoCYP82N5* and *CtoCYP82N6*) were clustered into one highly supported monophyletic group (Fig. 5b). For *CYP719* genes, two *C. sheareri* specific monophyletic groups were identified, consisting of three (*CshCYP719_01*, *CshCYP719_02,* and *CshCYP719_03*) and two members (*CshCYP719_04* and *CshCYP719_06*), respectively. Similarly, four members of *C. tomentella* clustered into two monophyletic groups in the phylogenetic tree (Fig. 5b).

Phylogenetic analysis of the *NCS* genes revealed four highly supported monophyletic clades (I–IV). In clade III, two *C. sheareri* specific monophyletic groups were identified, comprising seven (*CshNCS02*, *CshNCS03*, *CshNCS04*, *CshNCS05*, *CshNCS06*, *CshNCS16* and *CshNCS17*), and three (*CshNCS19*, *CshNCS20* and *CshNCS21*) members, respectively (Fig. 5c). In clade IV, one *C. sheareri* specific monophyletic group, and one *C. tomentella* specific monophyletic group were identified, containing three (*CshNCS07*, *CshNCS08* and *CshNCS09*) and two members (*CtoNCS4* and *CtoNCS9*), respectively (Fig. 5c).

Phylogeny the *CMT* genes revealed seven monophyletic clades (I–VII), and the majority of *Corydalis* members are scattered throughout the phylogenetic tree (Fig. 5d). Conversely, phylogenetic tree of the *NMT* genes revealed five highly supported clades (I–V) and eight species-specific monophyletic groups were recognized in *Corydalis* (Fig. 5e). In clade II, three species-specific monophyletic groups were identified, comprising four *C. sheareri* members (*CshNMT04*, *CshNMT05*, *CshNMT07,* and *CshNMT08*), four *C. tomentella* members (*CtoNMT14*, *CtoNMT15*, *CtoNMT16,* and *CtoNMT17*), and two *C. sheareri* members (*CshNMT19* and *CshNMT20*), respectively. In clade IV, four species-specific monophyletic groups, with three *C. sheareri* members (*CshNMT17*, *CshNMT21,* and *CshNMT22*), three *C. tomentella* members (*CtoNMT4*, *CtoNMT5,* and *CtoNMT6*), two *C. sheareri* members (*CshNMT14* and *CshNMT16*) and two *C. tomentella* members (*CtoNMT2* and *CtoNMT3*), respectively. In clade V, one monophyletic group, containing five *C. sheareri* members (*CshNMT10*, *CshNMT11*, *CshNMT12*, *CshNMT13,* and *CshNMT15*), was identified. Similarly, phylogenetic analysis of the *NMT* genes revealed eight well-supported clades (I–VIII). In clade III, three *C. tomentella* members (*Cto9OMT*, *CtoOMT10*, *CtoOMT11*) formed one well-supported monophyletic group. In clade VIII, another three *C. tomentella* members (*Cto6OMT*, *CtoOMT7*, and *CtoOMT8*) also formed one well-supported monophyletic group. While in clade V, two *C. sheareri* - specific monophyletic groups were identified, containing four (*CshOMT03*, *CshOMT04*, *CshOMT05,* and *CshOMT09*), and three (*CshOMT08*, *CshOMT10,* and *CshOMT11*) members, respectively.

Notably, the close relationship of the species-specific tandem duplicated gene pairs or clusters with high sequence similarity was confirmed in the phylogenetic analyses, such as *CshBBEL03* and its paralogs (*CshBBEL04* and *CshBBEL05*), *CshBBEL30* and its paralog *CshBBEL31*, *CshCYP719_01* and its paralogs (*CshCYP719_02* and *CshCYP719_03*), *CshNCS07* and its paralogs (*CshNCS08* and *CshNCS09*), *CshNCS19* and its paralogs (*CshNCS20* and *CshNCS21*), *CshNMT19* and its paralog *CshNMT20*, *CshTYR03* and its paralogs (*CshTYR04*, *CshTYR05,* and *CshTYR06*), *CtoCYP82N5* and its paralog *CtoCYP82N6*, and *CtoCYP719A2* and its paralog *CtoCYP719A2-2* (Fig. 5). The *Ka/Ks* ratio of these gene pairs ranged from 0.15543 to 0.43823 with an average of 0.292909 (Table 2), suggesting that purifying selection was the primary evolutionary force on these species-specific tandem duplicated gene pairs or clusters.

Discussion

Extremely complex tetraploid genome of *Corydalis sheareri*

In this study, by combining data from PacBio long-read sequencing, 3C-based Hi-C sequencing, and Illumina short-read sequencing, we assembled the genome of *Corydalis sheareri*, one species from subg. *Corydalis*, the largest and most diverse lineages of *Corydalis*. Genome survey showed that its genome is extremely complex (Fig. 1b). Both the GenomeScope and Smudgeplot analyses implied that the genome structure of *C. sheareri* might be an autotetraploid (a special tetraploid with three homologous chromosomes and one non-homologous chromosome) with a special AAAB karyotype (Fig. 1b, c). Intriguingly, the karyotype of *C. sheareri* is remarkably similar to that of *C. yanhusuo*[11], which also belongs to subg. *Corydalis*.

As previously reported, the diploid *C. tomentella* has a genome size of 258 Mb[12], and the estimated tetraploid *C. sheareri* genome size was 580 Mb (Supplementary Fig. S1a), which is nearly twice that of *C. tomentella*. This indicates that polyploidization might have played a significant role in the genome evolution within this genus. It is noteworthy that both *C. sheareri* and *C. yanhusuo* are tetraploid, yet their genome sizes differ by more than threefold. In *Corydalis*, both the genome size (https://cvalues.science.kew.org/search/angiosperm) and the chromosome number (https://ccdb.tau.ac.il/; http://legacy.tropicos.org/Project/IPCN) varied considerably. We deduce that diploidization following polyploidization, chromosomal rearrangements, including inversions, translocations, and changes in chromosome number via fusion and fission, as well as gene loss might be common and could thus trigger the genome size diversity in *Corydalis*. In our study, the detection of large-scale chromosomal structural variants, especially multiple inversions, between the genomes of *C. sheareri* and *C. tomentella* (Fig. 2e, f), seems to provide strong evidence in support of this hypothesis.

Tandem duplications drive the diversity of BIA biosynthetic genes in *Corydalis*

Polyploidization and structural variations might not only lead to changes in genome size but also substantially affect the gene content.

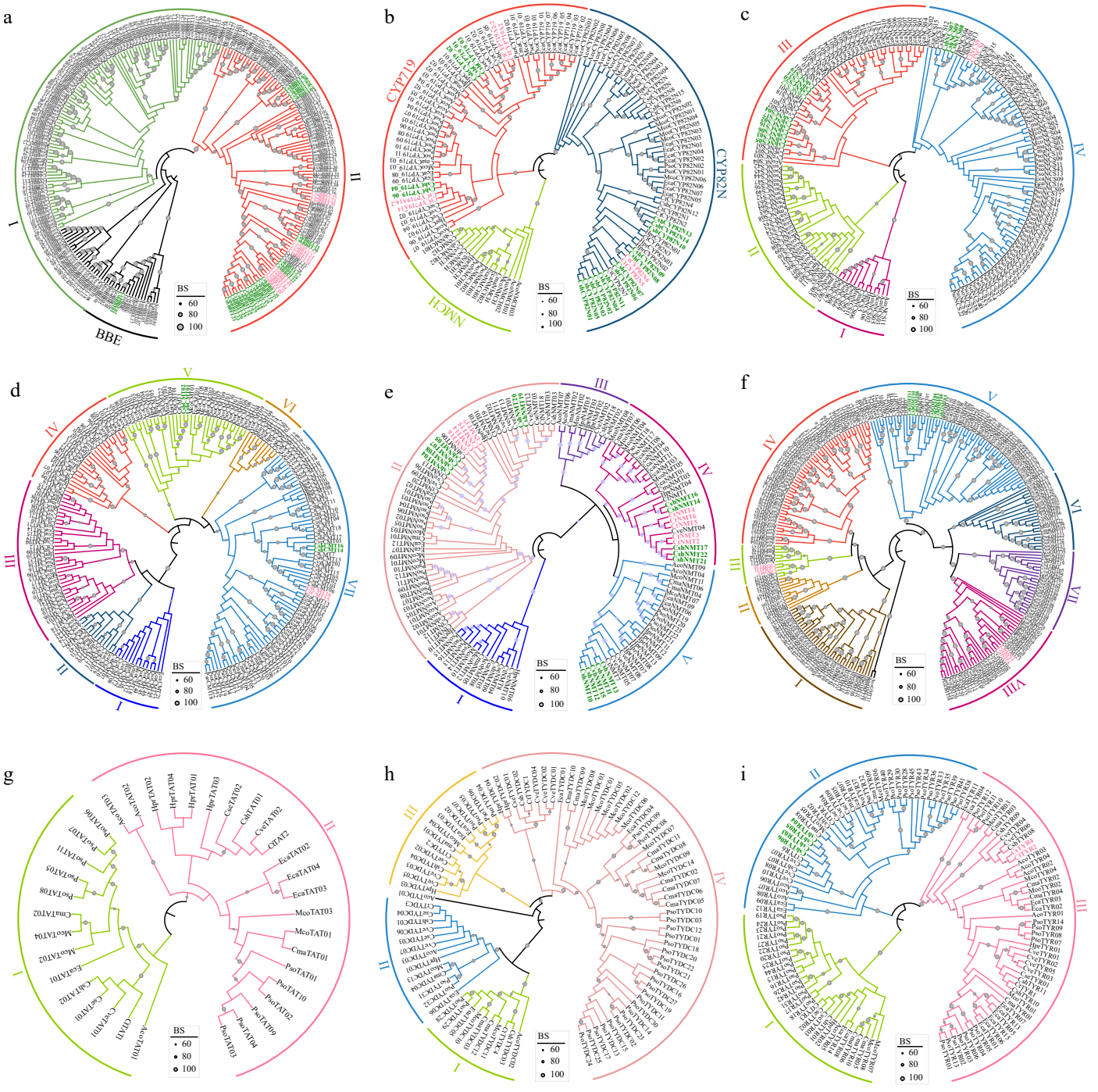

Fig. 5 Phylogenetic trees of BIAs biosynthesis genes. (a) *BBE* and *BBEL*, (b) *CYP719*, *CYP80B* (*NMCH*), and *CYP82N*, (c) *NCS*, (d) *CMT*, (e) *NMT*, (f) *OMT*, (g) *TAT*, (h) *TYDC*, and (i) *TYR*. *Corydalis shearei* and *C. tomentella* – specific monophyletic groups are highlighted with green and pink color, respectively. The gene and species abbreviations were the same as Fig. 3.

In this study, we identified 172 candidate genes involved in the BIAs biosynthesis within the *C. shearei* genome and traced their evolutionary history in Papaveraceae. As previously reported, BBELs, CMTs, NMTs, OMTs, and CYPs (CYP719, CYP82N) are the key enzymes downstream of the BIA biosynthetic pathway (Fig. 3a). In the *Corydalis* genome, the genes that encode these downstream enzymes, such as *BBEL*, *CMT*, *NMT*, and *OMT*, tend to possess a larger number of copies than the upstream genes of the BIA biosynthetic pathway (Fig. 3a, b), which enables plants to synthesize various BIAs. Interestingly, *NCS*, one upstream gene family, also has a relatively high copy number (Fig. 3b). NCS catalyzes the condensation of dopamine and 4-HPAA to produce norcoclaurine, which was identified as one of rate - limiting enzymes in BIA biosynthesis in opium poppy[62].

Furthermore, the chromosomal location and gene duplication analyses demonstrated that these genes frequently appeared as tandem duplications scattered throughout the genome (Figs 3c, 4). All these findings corroborated that tandem duplications might play a key role in the diversity of BIA biosynthetic genes in *Corydalis*. What's more, our comprehensive phylogenetic analyses, which cover representative species throughout Papaveraceae, revealed

Table 2. Selective pressure and sequence similarity of the species-specific tandem duplicated gene pairs or clusters in *Corydalis*.

Gene pairs or clusters	*Ka*	*Ks*	*Ka/Ks*	Similarity
CshBBEL03, *CshBBEL04*, *CshBBEL05*	0.1656	0.4321	0.38315	97.54%
CshBBEL30, *CshBBEL31*	0.1090	0.3349	0.32543	98.73%
CshCYP719_01, *CshCYP719_02*, *CshCYP719_03*	0.0841	0.3688	0.22803	98.81%
CshNCS07, *CshNCS08*, *CshNCS09*	0.0546	0.2236	0.24430	99.11%
CshNCS19, *CshNCS20*, *CshNCS21*	0.1325	0.8527	0.15543	94.61%
CshNMT19, *CshNMT20*	0.1435	0.4799	0.29900	98.68%
CshTYR03, *CshTYR04*, *CshTYR05*, *CshTYR06*	0.1635	0.373	0.43823	97.79%
CtCYP719A2, *CtCYP719A2-2*	0.0841	0.3808	0.22096	97.73%
CtCYP82N5, *CtCYP82N6*	0.0913	0.2672	0.34165	97.79%

that clade I and II of *NCS*, clades I, II, and VI of *CMT*, clades I and III of *NMT*, clades II, VI, and VII of *OMT*, two members of *TAT*, four members of *TYDC*, and clade I of *TYR*, each retain a single copy in *Corydalis* (Fig. 5). In addition, the fact that their homologs are shared by the majority of species suggests that they likely originate before the divergence of Papaveraceae or even Ranunculales. By contrast, the identification of *C. sheareri* or *C. tomentella* - specific monophyletic groups in *BBEL*, *CYP719*, *CYP82N*, clades III and IV of *NCS*, clades V and VI of *CMT*, clades II, IV and V of *NMT*, clades V and VIII of *OMT*, clade III of *TYR* (Fig. 5) indicate that recent gene duplications might occur frequently for these members in *Corydalis*. Particularly, the close relationship of some tandem duplicated gene pairs or clusters was confirmed in our phylogenetic analyses (Fig. 5), strongly suggesting that these genes may be generated from the recent duplication events that occurred within *C. sheareri,* or *C. tomentella.* Additionally, more *C. sheareri*-specific tandem duplication events are identified compared to those in *C. tomentella*, which is likely associated with the significant expansion of BIAs biosynthetic genes in *C. sheareri.*

Until recently, with the burst of plant genome sequencing projects and the advancement of bioinformatic tools, biosynthetic pathways for many natural products have been elucidated[63–65]. Numerous studies have stated that tandem duplication is a major factor contributing to the diversity of secondary metabolites biosynthesis, by recruiting novel genes and potentially introducing new metabolic pathways. For instance, *Papaver somniferum* has undergone significant tandem duplication events, which result in the emergence of morphinan and noscapine biosynthesis pathways[22,66]. The divergence and expansion of *CYP* genes strongly contribute to the alkaloid diversity in *Coptis*[67]. Tandem duplications are also common for the triterpene biosynthetic genes in *Aralia elata*, especially for *CYP72A*, *CSLM*, and *UGT73*, which may drive the diversity of triterpenoids[68]. In the case of *Scutellaria*, tandem duplications of the CYP82D subfamily shape the flavonoid diversification[69]. In *Corydalis*, each species was found to contain a particular set of BIAs, some of which are common to other species but not in the same combinations. *BBEL* genes have been reported to be expanded and considered to be related to the appearance of cavidines and coptisine in *C. tomentella*[12]. In this study, tandem duplications are also found to be evident in other genes involved in the biosynthesis of BIAs, particularly *NCS*, *CMT*, *NMT*, *OMT,* and *CYP*. Despite not conducting the functional experiment, we still have reason to believe that tandem duplications may drive the expansion of BIA biosynthesis genes, which is conducive to the complexity of biosynthesis pathway and further contributes the BIAs diversity in *Corydalis*. The incorporation of sequencing data from more *Corydalis* species, in conjunction with the conduction of multi-omics landscape investigations and the performance of functional experiment studies related to these recently duplicated genes in the future, may lead to an updated canvas for illustrating the genetic mechanisms underlying the diversity of BIAs.

Conclusions

In this study, we proposed that *C. sheareri* might be a complex autotetraploid with a special AAAB karyotype. Genomic comparison detected large syntenic blocks between *C. sheareri* and its relatives *C. tomentella*, and also uncovered large-scale chromosomal structural variations (particularly inversions) between these two genomes, which might have profound effects on the divergence of *Corydalis*. Furthermore, we identified 172 candidate genes involved in BIAs biosynthesis in *C. sheareri* and traced their evolution history in Papaveraceae. We deduce that tandem duplication has played a prominent role in the expansion of the BIAs biosynthesis genes, especially for *BBEL*, *CMT*, *NMT*, *OMT*, and *NCS*. Moreover, the identification of the species-specific tandem duplication events implies that the growth in the number of gene members is likely to complicate the metabolic pathway, and consequently, has further contributed to the diversification of BIAs biosynthesis, ultimately leading to the diversity of BIAs in *Corydalis*. Our study provides more insights into the genome evolution for species-rich taxa with radiation, as well as the mechanisms underlying the diversity of the BIA biosynthetic pathway. It is also of great value for future genetic studies and medicinal applications of *Corydalis*.

Author contributions

The authors confirm contribution to the paper as follows: study conception and design: Liu YY, Peng D, Li JM; data collection: Liu YY, Peng D, Yu CL, Liu YJ, Chen M, Kan SL, Cao YN; analysis and interpretation of results: Liu YY, Peng D, Yu CL, Liu YJ, Kan SL, Cao YN; draft manuscript preparation: Liu YY, Peng D, Wang HW, Li JM, Peng D. All authors reviewed the results and approved the final version of the manuscript.

Data availability

The whole-genome sequence data, including Illumina short reads, PacBio HiFi reads, Hi-C interaction reads, transcriptome data, and genome annotation files, have been deposited in The National Genomics Data Center (NGDC), under the project number: PRJCA035358.

Acknowledgments

We thank Dr Yuan-Yuan Feng (Institute of Botany, Chinese Academy of Sciences) for her help in the flow cytometry measurement. We also thank Mr Hai-Kuan Zhang (Berry Genomics Company) for his help in the genome assembly and annotation. This research was funded by National Natural Science Foundation of China (32000170) and Xinyang Academy of Ecological Research Open Foundation (2023XYMS05).

Conflict of interest

The authors declare that they have no conflict of interest.

Supplementary information accompanies this paper at (https://www.maxapress.com/article/doi/10.48130/gcomm-0025-0002)

Dates

Received 26 November 2024; Revised 20 January 2025; Accepted 22 January 2025; Published online 25 February 2025

References

1. Chen JT, Lidén M, Huang XH, Zhang L, Zhang XJ, et al. 2023. An updated classification for the hyper-diverse genus *Corydalis* (Papaveraceae: Fumarioideae) based on phylogenomic and morphological evidence. *Journal of Integrative Plant Biology* 65:2138–56
2. Wu ZY, Zhuang X, Su ZY. 1999. *Corydalis* DC. In *Flora Reipublicae Popularis Sinicae*, ed. Wu ZY. Volume 32. Beijing: Science Press
3. Zhang ML, Su ZY, Lidén M. 2008. *Corydalis* DC. In *Flora of China*, eds., Wu ZY, Raven PH, Hong DY. Volume 7. Beijing: Science Press and St. Louis, MO: Missouri Botanical Garden Press
4. Pérez-Gutiérrez MA, Romero-García AT, Fernández MC, Blanca G, Salinas-Bonillo MJ, et al. 2015. Evolutionary history of fumitories (subfamily Fumarioideae, Papaveraceae): an old story shaped by the main geological and climatic events in the Northern Hemisphere. *Molecular Phylogenetics and Evolution* 88:75–92
5. Peng HW, Xiang KL, Erst AS, Lian L, Ortiz RDC, et al. 2023. A complete genus-level phylogeny reveals the Cretaceous biogeographic diversification of the poppy family. *Molecular Phylogenetics and Evolution* 181:107712
6. Peng HW, Xiang KL, Erst AS, Erst TV, Jabbour F, et al. 2023. The synergy of abiotic and biotic factors correlated with diversification of Fumarioideae (Papaveraceae) in the Cenozoic. *Molecular Phylogenetics and Evolution* 186:107868
7. Liu YY, Cao JL, Kan SL, Wang PH, Wang JL, et al. 2024. Phylogenomic analyses sheds new light on the phylogeny and diversification of *Corydalis* DC. in Himalaya-Hengduan Mountains and adjacent regions. *Molecular Phylogenetics and Evolution* 193:108023
8. Zou Y, Wang J, Peng D, Zhang X, Tembrock LR, et al. 2023. Multi-integrated genomic data for *Passiflora foetida* provides insights into genome size evolution and floral development in *Passiflora*. *Molecular Horticulture* 3:27
9. Lan L, Leng L, Liu W, Ren Y, Reeve W, et al. 2024. The haplotype-resolved telomere-to-telomere carnation (*Dianthus caryophyllus*) genome reveals the correlation between genome architecture and gene expression. *Horticulture Research* 11:uhad244
10. Xia XM, Du HL, Hu XD, Wu JJ, Yang FS, et al. 2024. Genomic insights into adaptive evolution of the species-rich cosmopolitan plant genus *Rhododendron*. *Cell Reports* 43:114745
11. Xu D, Ye Z, Huang Y, Zhu K, Xu H, et al. 2024. Haplotype-resolved genome assembly of *Corydalis yanhusuo*, a traditional Chinese medicine with unusual telomere motif. *Horticulture Research* 11:uhad296
12. Xu Z, Li Z, Ren F, Gao R, Wang Z, et al. 2022. The genome of *Corydalis* reveals the evolution of benzylisoquinoline alkaloid biosynthesis in Ranunculales. *Plant Journal* 111:217–30
13. Deng AP, Zhang Y, Zhou L, Kang CZ, Lv CG, et al. 2021. Systematic review of the alkaloid constituents in several important medicinal plants of the genus *Corydalis*. *Phytochemistry* 183:112644
14. Fu XY, Liang WZ, Tu GS. 1986. Alkaloid from dongyang corydalis yanhusuo. *Acta Pharmaceutica Sinica B* 21:447–53
15. Hussain SF, Siddiqui MT. 1992. Alkaloidal constituents of *Corydalis stewartii*. *Planta Medica* 58:108
16. Xu D, Lin H, Tang Y, Huang L, Xu J, et al. 2021. Integration of full-length transcriptomics and targeted metabolomics to identify benzylisoquinoline alkaloid biosynthetic genes in *Corydalis yanhusuo*. *Horticulture Research* 8:16
17. Zhao X, Pan Y, Tan J, Lv H, Wang Y, et al. 2024. Metabolomics and transcriptomics reveal the mechanism of alkaloid synthesis in *Corydalis yanhusuo* bulbs. *PLoS ONE* 19:e0304258
18. Liu X, Liu Y, Huang P, Ma Y, Qing Z, et al. 2017. The genome of medicinal plant *Macleaya cordata* provides new insights into benzylisoquinoline alkaloids metabolism. *Molecular Plant* 10:975–89
19. Yamada Y, Hirakawa H, Hori K, Minakuchi Y, Toyoda A, et al. 2021. Comparative analysis using the draft genome sequence of California poppy (*Eschscholzia californica*) for exploring the candidate genes involved in benzylisoquinoline alkaloid biosynthesis. *Bioscience, Biotechnology, and Biochemistry* 85:851–59
20. Desgagné-Penix I, Facchini PJ. 2012. Systematic silencing of benzylisoquinoline alkaloid biosynthetic genes reveals the major route to papaverine in opium poppy. *The Plant Journal* 72:331–44
21. Singh A, Menéndez-Perdomo IM, Facchini PJ. 2019. Benzylisoquinoline alkaloid biosynthesis in opium poppy: an update. *Phytochemistry Reviews* 18:1457–82
22. Guo L, Winzer T, Yang X, Li Y, Ning Z, et al. 2018. The opium poppy genome and morphinan production. *Science* 362:343–47
23. Chen S, Zhou Y, Chen Y, Gu J. 2018. fastp: an ultra-fast all-in-one FASTQ preprocessor. *Bioinformatics* 34(17):i884–90
24. Dolezel J, Bartos J. 2005. Plant DNA flow cytometry and estimation of nuclear genome size. *Annals of Botany* 95:99–110
25. Kokot M, Dlugosz M, Deorowicz S. 2017. KMC 3: counting and manipulating *k-mer* statistics. *Bioinformatics* 33:2759–61
26. Rhyker Ranallo-Benavidez T, Jaron KS, Schatz MC. 2020. GenomeScope 2.0 and Smudgeplot for reference-free profiling of polyploid genomes. *Nature Communications* 11:1432
27. Cheng H, Concepcion GT, Feng X, Zhang H, Li H. 2021. Haplotype resolved de-novo assembly using phased assembly graphs with hifiasm. *Nature Methods* 18:170–75
28. Guan D, McCarthy SA, Wood J, Howe K, Wang YD, et al. 2020. Identifying and removing haplotypic duplication in primary genome assemblies. *Bioinformatics* 36:2896–98
29. Durand NC, Shamim MS, Machol I, Rao SSP, Huntley MH, et al. 2016. Juicer provides a one-click system for analyzing loop-resolution Hi-C experiments. *Cell Systems* 3:95–98
30. Dudchenko O, Batra SS, Omer AD, Nyquist SK, Hoeger M, et al. 2017. De novo assembly of the *Aedes aegypti* genome using Hi-C yields chromosome-length scaffolds. *Science* 356:92–95
31. Durand NC, Robinson JT, Shamim MS, Machol I, Mesirov JP, et al. 2016. Juicebox provides a visualization system for Hi-C contact maps with unlimited zoom. *Cell Systems* 3:99–101
32. Li H, Durbin R. 2009. Fast and accurate short read alignment with Burrows-Wheeler transform. *Bioinformatics* 25:1754–60
33. Li H. 2018. Minimap2: pairwise alignment for nucleotide sequences. *Bioinformatics* 34(18):3094–100
34. Manni M, Berkeley MR, Seppey M, Zdobnov EM. 2021. BUSCO: Assessing genomic data quality and beyond. *Current Protocols* 1:e323
35. Xu Z, Wang H. 2007. LTR_FINDER: an efficient tool for the prediction of full-length LTR retrotransposons. *Nucleic Acids Research* 35:W265–W268
36. Han Y, Wessler SR. 2010. MITE-hunter: a program for discovering miniature inverted-repeat transposable elements from genomic sequences. *Nucleic Acids Research* 38:e199
37. Stanke M, Keller O, Gunduz I, Hayes A, Waack S, et al. 2006. AUGUSTUS: ab initio prediction of alternative transcripts. *Nucleic Acids Research* 34:W435–W439
38. Korf I. 2004. Gene finding in novel genomes. *BMC Bioinformatics* 5:59
39. Majoros WH, Pertea M, Salzberg SL. 2004. TigrScan and GlimmerHMM: two open source *ab initio* eukaryotic gene-finders. *Bioinformatics* 20:2878–79
40. Lomsadze A, Burns PD, Borodovsky M. 2014. Integration of mapped RNA-Seq reads into automatic training of eukaryotic gene finding algorithm. *Nucleic Acids Research* 42:e119
41. Keilwagen J, Hartung F, Grau J. 2019. GeMoMa: Homology-based gene prediction utilizing intron position conservation and RNA-seq data. *Methods in Molecular Biology* 1962:161–77
42. Grabherr MG, Haas BJ, Yassour M, Levin JZ, Thompson DA, et al. 2011. Full-length transcriptome assembly from RNA-Seq data without a reference genome. *Nature Biotechnology* 29:644–52
43. Haas BJ, Delcher AL, Mount SM, Wortman JR, Smith RK Jr, et al. 2003. Improving the *Arabidopsis* genome annotation using maximal transcript alignment assemblies. *Nucleic Acids Research* 31:5654–66
44. Lowe TM, Eddy SR. 1997. tRNAscan-SE: a program for improved detection of transfer RNA genes in genomic sequence. *Nucleic Acids Research* 25:955–64

45. Emms DM, Kelly S. 2015. OrthoFinder: solving fundamental biases in whole genome comparisons dramatically improves orthogroup inference accuracy. *Genome Biology* 16:157
46. Katoh K, Standley DM. 2013. MAFFT multiple sequence alignment software version 7: improvements in performance and usability. *Molecular Biology and Evolution* 30:772–80
47. Stamatakis A. 2014. RAxML Version 8: a tool for phylogenetic analysis and post-analysis of large phylogenies. *Bioinformatics* 30:1312–13
48. Yang Z. 2007. PAML 4: phylogenetic analysis by maximum likelihood. *Molecular Biology and Evolution* 24:1586–91
49. De Bie T, Cristianini N, Demuth JP, Hahn MW. 2006. CAFE: a computational tool for the study of gene family evolution. *Bioinformatics* 22:1269–71
50. Sun P, Jiao B, Yang Y, Shan L, Li T, et al. 2022. WGDI: a user-friendly toolkit for evolutionary analyses of whole-genome duplications and ancestral karyotypes. *Molecular Plant* 15:1841–51
51. Wang Y, Tang H, DeBarry JD, Tan X, Li J, et al. 2012. *MCScanX*: A toolkit for detection and evolutionary analysis of gene synteny and collinearity. *Nucleic Acids Research* 40:e49
52. Tang H, Krishnakumar V, Zeng X, Xu Z, Taranto A, et al. 2024. JCVI: A versatile toolkit for comparative genomics analysis. *iMeta* 3:e211
53. Chen C, Chen H, Zhang Y, Thomas HR, Frank MH, et al. 2020. TBtools: an integrative toolkit developed for interactive analyses of big biological data. *Molecular Plant* 13:1194–202
54. Goel M, Sun H, Jiao WB, Schneeberger K. 2019. SyRI: finding genomic rearrangements and local sequence differences from whole-genome assemblies. *Genome Biology* 20(1):277
55. Jiao YN, Wickett NJ, Ayyampalayam S, Chanderbali AS, Landherr L, et al. 2011. Ancestral polyploidy in seed plants and angiosperms. *Nature* 473:97–100
56. Nguyen LT, Schmidt HA, von Haeseler A, Minh BQ. 2015. IQ-TREE: A fast and effective stochastic algorithm for estimating maximum-likelihood phylogenies. *Molecular Biology and Evolution* 32:268–74
57. The French–Italian Public Consortium for Grapevine Genome Characterization. 2007. The grapevine genome sequence suggests ancestral hexaploidization in major angiosperm phyla. *Nature* 449:463–67
58. Amborella Genome Project. The Amborella genome and the evolution of flowering plants. *Science* 2013: 342
59. Thorvaldsdóttir H, Robinson JT, Mesirov JP. 2013. Integrative Genomics Viewer (IGV): high-performance genomics data visualization and exploration. *Briefings in Bioinformatics* 14(2):178–92
60. Ikezawa N, Iwasa K, Sato F. 2009. CYP719A subfamily of cytochrome P450 oxygenases and isoquinoline alkaloid biosynthesis in *Eschscholzia californica*. *Plant Cell Reports* 28:123–33
61. Hori K, Yamada Y, Purwanto R, Minakuchi Y, Toyoda A, et al. 2018. Mining of the uncharacterized cytochrome *P450* genes involved in alkaloid biosynthesis in California poppy using a draft genome sequence. *Plant and Cell Physiology* 59:222–33
62. Samanani N, Facchini PJ. 2001. Isolation and partial characterization of norcoclaurine synthase, the first committed step in benzylisoquinoline alkaloid biosynthesis, from opium poppy. *Planta* 213:898–906
63. Huang H, Liang J, Tan Q, Ou L, Li X, et al. 2021. Insights into triterpene synthesis and unsaturated fatty-acid accumulation provided by chromosomal-level genome analysis of *Akebia trifoliata* subsp. *australis*. *Horticulture Research* 8:33
64. Jiang Z, Tu L, Yang W, Zhang Y, Hu T, et al. 2021. The chromosome-level reference genome assembly for *Panax notoginseng* and insights into ginsenoside biosynthesis. *Plant Communications* 2:100113
65. Han X, Li C, Sun S, Ji J, Nie B, et al. 2022. The chromosome-level genome of female ginseng (*Angelica sinensis*) provides insights into molecular mechanisms and evolution of coumarin biosynthesis. *The Plant Journal* 112:1224–37
66. Yang X, Gao S, Guo L, Wang B, Jia Y, et al. 2021. Three chromosome-scale *Papaver* genomes reveal punctuated patchwork evolution of the morphinan and noscapine biosynthesis pathway. *Nature Communications* 12:6030
67. Liu Y, Wang B, Shu S, Li Z, Song C, et al. 2021. Analysis of the *Coptis chinensis* genome reveals the diversification of protoberberine-type alkaloids. *Nature Communications* 12:3276
68. Wang Y, Zhang H, Ri HC, An ZY, Wang X, et al. 2022. Deletion and tandem duplications of biosynthetic genes drive the diversity of triterpenoids in *Aralia elata*. *Nature Communications* 13:2224
69. Qiu S, Wang J, Pei T, Gao R, Xiang C, et al. 2025. Functional evolution and diversification of the CYP82D subfamily members shape flavonoid diversification in the genus *Scutellaria*. *Plant Communications* 6:101134